

Multifractality and polygonal vortex filaments

VALERIA BANICA
DANIEL ECEIZABARRENA
ANDREA R. NAHMOD
LUIS VEGA

ABSTRACT. In this proceedings article we survey the results in [5] and their motivation, as presented at the 50th Séminaire *Équations aux dérivées partielles* 2024. With the aim of quantifying turbulent behaviors of vortex filaments, we study the multifractality of a family of generalized Riemann's non-differentiable functions. These functions represent, in a certain limit, the trajectory of regular polygonal vortex filaments that evolve according to the binormal flow, the classical model for vortex filaments dynamics. We explain how we determined their spectrum of singularities through a careful design of Diophantine sets, which we study by using the Duffin-Schaeffer theorem and the Mass Transference Principle.

Multifractalité et des tourbillons filamentaires polygonaux

RÉSUMÉ. Dans cet acte de conférence nous passons en revue les résultats de [5] et leur motivation, tels qu'ils ont été présentés au 50e Séminaire *Équations aux dérivées partielles* 2024. Dans le but de quantifier les comportements turbulents des filaments tourbillonnaires, nous étudions la multifractalité d'une famille de fonctions non différentiables de Riemann généralisées. Ces fonctions représentent, dans une certaine limite, la trajectoire de filaments tourbillonnaires polygonaux réguliers qui évoluent selon le flot binormal, le modèle classique pour la dynamique des tourbillons filamentaires. Nous expliquons comment nous avons déterminé pour certaines de ces fonctions le spectre des singularités. La preuve repose sur une construction d'ensembles diophantiens que nous étudions en utilisant le théorème de Duffin-Schaeffer et le principe de transfert de masse.

1. Multifractal analysis and Riemann's non-differentiable function

Multifractal analysis started in the 1980s to explain the deviations from Kolmogorov's 1941 theory of turbulence observed by Anselmet et al. [1] (see Arneodo and Jaffard's expository article [4]). In these experiments, the speed of the turbulent fluid seems very irregular in some regions and less in others, and the borders between regions are unclear. What is more, zooming in very irregular regions one finds less irregular regions, and vice-versa. Facing such a non-uniform distribution of regularities, instead of explicitly computing the

V.B. is partially supported by the French ANR grant BOURGEONS and by the ERC grant GEOEDP. D.E. is partially supported by the European Union Horizon Europe research and innovation programme under Marie Skłodowska Curie Actions with grant agreement 101104250 - TIDE, by the Simons Foundation Collaboration Grant on Wave Turbulence (Nahmod's award ID 651469), and by the American Mathematical Society and the Simons Foundation under an AMS-Simons Travel Grant for the period 2022-2024.

A.N. is partially supported by NSF DMS-2052740, NSF DMS-2101381 and the Simons Foundation Collaboration Grant on Wave Turbulence (Nahmod's award ID 651469).

L.V. is partially supported by MICINN (Spain) CEX2021-001142, PID2021-126813NB-I00 (ERDF A way of making Europe) and IT1247-19 (Gobierno Vasco).

Keywords: Vortex filaments, multifractality, Riemann's non-differentiable function, Diophantine approximation.

2020 Mathematics Subject Classification: 11J82, 11J83, 26A27, 28A78, 42A16, 76F99.

regularity at each individual point it turns out that it is more suitable to measure the sets where a given regularity is reached. A typical way to formalize this is as follows.

For $f : \mathbb{R} \rightarrow \mathbb{R}$ and $0 < \alpha < 1$, the local Hölder regularity of f at a point t is measured as

$$f \in \mathcal{C}^\alpha(t) \iff |f(t+h) - f(t)| \leq Ch^\alpha, \quad \forall h \ll 1,$$

and the local Hölder exponent of f at a point t is given by

$$\alpha_f(t) = \sup\{\alpha : f \in \mathcal{C}^\alpha(t)\}.$$

A multifractal function is a function possessing infinitely many local Hölder exponents. The multifractal analysis of a function consists in computing its spectrum of singularities, that is, the Hausdorff dimension¹ of its iso-Hölder sets

$$d_f(\alpha) = \dim_{\mathcal{H}}\{t : \alpha_f(t) = \alpha\}.$$

By convention, we set $d_f(\alpha) = -\infty$ if the set $\{t : \alpha_f(t) = \alpha\}$ is empty.

A classical example of multifractal function is

$$R(t) = \sum_{n=1}^{\infty} \frac{\sin(n^2 t)}{n^2},$$

proposed by Riemann in 1860 when he was looking for continuous functions that are nowhere differentiable. Weierstrass, who failed to prove the claim that R is actually nowhere differentiable (which eventually turned out to be false!), proved that the function

$$W(t) = \sum_{n=1}^{\infty} \frac{\cos(4^n t)}{2^n},$$

which is simpler to study, is nowhere differentiable. However, it is not multifractal because it has Hölder exponent $1/2$ everywhere; it is rather a *monofractal* function. In particular, its spectrum of singularity is

$$d_W(\alpha) = \begin{cases} 1, & \alpha = 1/2, \\ -\infty, & \alpha \neq 1/2. \end{cases}$$

Riemann's function is richer; Hardy [35] and Gerver [31, 32] showed that it actually allows a derivative at certain points, and it was proved by Jaffard [37] to be a genuine multifractal function with spectrum of singularities

$$d_R(\alpha) = \begin{cases} 4\alpha - 2, & 1/2 \leq \alpha \leq 3/4, \\ 0, & \alpha = 3/2, \\ -\infty, & \text{otherwise,} \end{cases}$$

a result that holds too for its complex version given by the function

$$R_0(t) = \sum_{n \in \mathbb{Z} \setminus \{0\}} \frac{e^{in^2 t}}{n^2}.$$

Jaffard actually computed the local Hölder regularity at every point, a result for which Broucke and Vindas [15] gave recently an alternative proof.

Other notions related to turbulence were successfully tested on Riemann's function. Jaffard [37] showed that it satisfies the Frisch-Parisi multifractal formalism (see (2.3)),

¹We recall that the s -Hausdorff measure of a set is

$$\mathcal{H}^s(A) = \lim_{\delta \rightarrow 0} \left(\inf \left\{ \sum_{j=1}^{\infty} \text{diam}(A_j)^s : A \subset \bigcup_{j=1}^{\infty} A_j, \text{diam}(A_j) < \delta \right\} \right),$$

and the Hausdorff dimension of a set A is

$$\dim_{\mathcal{H}} A = \sup\{s : \mathcal{H}^s(A) = \infty\} = \inf\{s : \mathcal{H}^s(A) = 0\}.$$

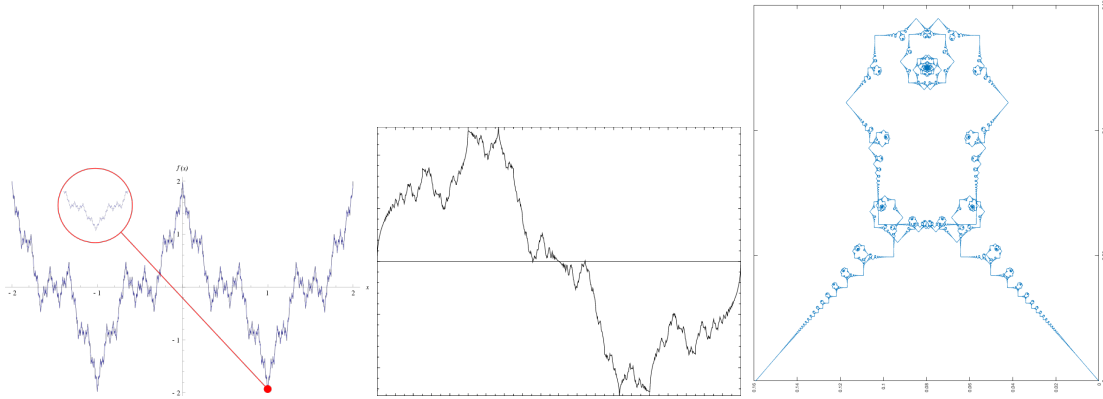


FIGURE 1. The graphs of W , R , and the image of \tilde{R}_0 .

and Boritchev, Vilaça Da Rocha and Eceizabarrena [14] proved that it is intermittent (see (2.2)). Also, Eceizabarrena [26, 27] showed that the image of R_0 has no tangents and has Hausdorff dimension² less than $4/3$.

Generalizations of Riemann's function were intensively studied after the work of Jaffard. For example, Chamizo and Ubis [16], and Seuret and Ubis [43] obtained upper and lower bounds for the spectrum of singularities of $\sum_n \frac{e^{iP(n)t}}{n^\alpha}$ with P a polynomial, with an approach different from Jaffard's wavelet techniques and the unimodular group action on Riemann's function. Vilaça Da Rocha and Eceizabarrena [28] studied the intermittency of $\sum_n \frac{e^{in^2t}}{n^\alpha}$ with $\alpha > 1/2$. Kapitanski and Rodnianski [40] gave fine regularity results for $\sum_n e^{in^2t_0+inx}$ with t_0 fixed, which represents the fundamental solution to the periodic Schrödinger equation at time t_0 . Banica and Vega [7] proved that the spectrum of singularities of $\sum_{n \in \mathbb{N}} \frac{e^{i(pn+q)^2t}}{(pn+q)^2}$ for $p, q \in \mathbb{N}$ is the same as for Riemann's function, and that the Frisch-Parisi multifractal formalism is also satisfied.

2. Main result

In [5] we study a different generalization of the Riemann function, namely

$$R_{x_0}(t) = \sum_{n \in \mathbb{Z} \setminus \{0\}} \frac{e^{2\pi i(n^2t + nx_0)}}{n^2}, \quad \text{for } x_0 \text{ fixed.}$$

These functions, or rather the closely related³

$$\tilde{R}_{x_0}(t) = \sum_{n \in \mathbb{Z}} \frac{e^{in^2t} - 1}{n^2} e^{inx_0},$$

arise naturally in the setting of vortex filaments, as we explain in Section 3. In Figure 2 we display the images of \tilde{R}_{x_0} for different values of x_0 . The result from [5] that we here review is the following.

²Note that even the Hausdorff dimension of the graph of the Weierstrass function was determined only recently by Shen [44]

³In particular, the functions R_{x_0} and \tilde{R}_{x_0} have the same regularity in t .

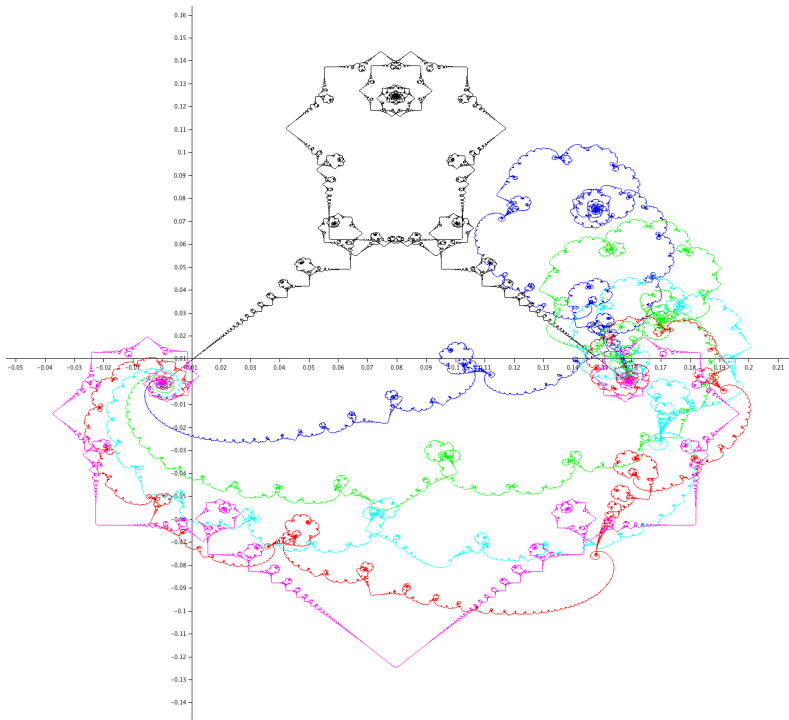


FIGURE 2. The curve $\tilde{R}_{x_0}([0, 2\pi])$ for several values of x_0 : 0 (black), 0.1 (blue), 0.2 (green), 0.3 (cyan), 0.4 (red), 0.5 (magenta).

Theorem 1. *Let $x_0 \in \mathbb{R}$. Then, the function R_{x_0} is multifractal, with infinitely many local Hölder exponents. If $x_0 \in \mathbb{Q}$, the spectrum of singularities of R_{x_0} is*

$$d_{R_{x_0}}(\alpha) = \begin{cases} 4\alpha - 2, & 1/2 \leq \alpha \leq 3/4, \\ 0, & \alpha = 3/2, \\ -\infty, & \text{otherwise.} \end{cases} \quad (2.1)$$

The proof starts as in Jaffard's [37] and then it follows the approach by Chamizo and Ubis in [16], but it ends up with new Diophantine sets that approximate the iso-Hölder sets. We measure these new sets combining the Duffin-Schaeffer theorem⁴ [25] and the Beresnevich-Velani Mass Transference Principle [13]. We explain this procedure in detail in Section 4.

In [5] we also showed that R_{x_0} is intermittent in small scales by proving that its flatness tends to infinity when the scale parameter tends to zero, that is,

$$F_{R_{x_0}}(N) := \frac{\|P_{\geq N} R_{x_0}\|_4^4}{\|P_{\geq N} R_{x_0}\|_2^4} \xrightarrow{N \rightarrow \infty} \infty, \quad (2.2)$$

where $P_{\geq N}$ is the high-pass filter of Fourier modes larger than N . As a consequence, one can deduce that the function satisfies the Frisch-Parisi multifractal formalism⁵

$$d_{R_{x_0}}(\alpha) = \inf_p \{ \alpha p - \eta_{R_{x_0}}(p) + 1 \}, \quad \text{for } \frac{1}{2} \leq \alpha \leq \frac{3}{4}, \quad (2.3)$$

⁴The Duffin-Schaeffer theorem was conjectured by Duffin and Schaeffer [25] in 1941, and they proved it in some particular cases that suffice to prove Theorem 1 for $x_0 \in \mathbb{Q}$. It was recently proved in all generality by Koukoulopoulos and Maynard [42], which we need for our results in [5] when $x_0 \notin \mathbb{Q}$.

⁵The Frisch-Parisi multifractal formalism was originally proposed for the velocity in an Eulerian setting, but it can be equally proposed in the Lagrangian setting, which Riemann's function is in principle more related to since it represents a time trajectory. See the work of Chevillard et al. [17] for a discussion on the differences between these two frameworks.

where $\eta_{R_{x_0}}(p) := \sup\{s, R_{x_0} \in B_{p,\infty}^{s/p}\}$ and $B_{p,\infty}^{s/p}$ stands for the Besov space⁶.

Regarding the case when x_0 is irrational, we proved that R_{x_0} is multifractal by giving a result on its spectrum of singularities, although not recovering it explicitly. The difficulty comes from the interference between the exponents of irrationality of both x_0 and t .

3. Motivation from fluid dynamics

In this section we explain how Riemann's function R_{x_0} appears naturally in the evolution of curves that evolve according to the binormal flow model for vortex filaments dynamics. Let us first recall this model and some very recent results related to it.

3.1. The binormal flow

The binormal flow (BF), also known as local induction approximation (LIA) or vortex filament equation (VFE), is the oldest, simplest and richest formally derived model for one vortex filament dynamics in a 3D fluid governed by Euler's equations. If the vorticity at time t is concentrated along an arclength-parametrized curve $\chi(t)$ in \mathbb{R}^3 , its evolution in time is expected to evolve according to the equation

$$\chi_t = \chi_x \times \chi_{xx}, \quad \text{or equivalently} \quad \chi_t = cb, \quad (3.1)$$

where b is the binormal vector of the curve χ and c is its curvature. This model was derived formally from the Biot-Savart formula by Da Rios in 1906 [19], and it was justified rigorously by Jerrard and Seis in 2017 [38]. Understanding if and when the vorticity propagates its initial structure of being concentrated along a curve is still a very difficult open problem.

Let us briefly recall a few very recent advances in this direction. Concerning the Navier-Stokes equation, Bedrossian, Germain and Harrop-Griffiths [12] proved that the Cauchy problem is locally well-posed for an initial filament data with no symmetry assumptions, but for times that are too small to observe the binormal flow and to pass to the vanishing viscosity limit. The vanishing viscosity limit was proved by Gallay and Sverak [30] for the particular case of axisymmetric vortex rings. The BF dynamics was recovered by Fontelos and Vega [29] for Giga-Miyakawa solutions with initial filament data with no symmetry assumptions, but this regime does not allow to pass to the vanishing viscosity limit. For the Euler equations Donati, Lacave and Miot [24], and previously Dávila, Del Pino, Musso and Wei [20] with other methods, constructed solutions with vorticity concentrated on helices, which are particular solutions of the binormal flow. These are configurations with symmetries benefitting from a dimensional reduction. Thus, despite recent efforts, the binormal flow conjecture is still a serious gap away from being understood.

3.2. Experiments, numerics, and a rigorous result

A special class of solutions of the binormal flow are the self-similar solutions, which are smooth curves that develop a singularity in the shape of a corner in finite time. They were known and used by physicists since the 1980s in the framework of reconnection of vortex filaments in ferromagnetics, but they were not rigorously studied until 2003 by Gutiérrez, Rivas and Vega [34]. This type of dynamics appears in fluids passing over a triangular obstacle and in trail vortex reconnection, as shown in Figure 3 left. The interaction of many corner singularities yields a range of complex behaviors such as the Talbot effect,

⁶See the recent works by Barral and Seuret [10, 11] on the validity of the multifractal formalism in Besov spaces.

L^∞ -cascades of energy, rogue waves, intermittency and multifractal behaviors [5, 6, 7, 8, 9]. Here we consider the last type of results that are the object of this proceedings article.

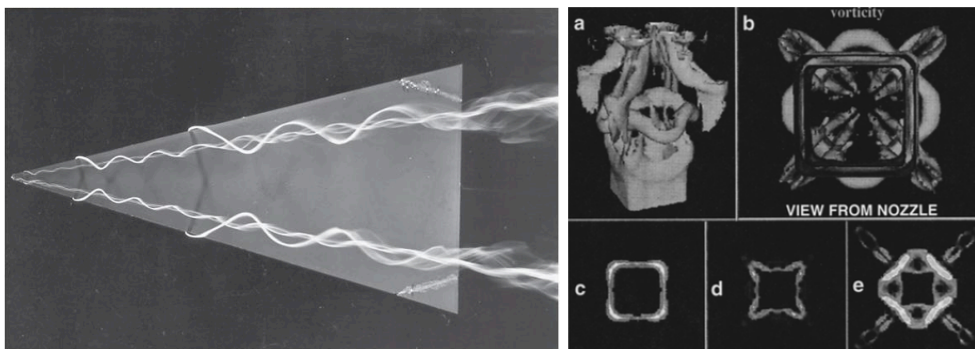


FIGURE 3. On the left: vortices in a fluid flowing over a triangular obstacle. On the right: axis switching in numerical simulation of square jets.

Noncircular jets such as square jets have been studied since the 1980s for the turbulent features they produce. The experiments by Todoya and Hussain [45] and the numerics by Grinstein and De Vore [33] are some examples of this, see Figure 3 right. At the level of the binormal flow this corresponds to considering as initial data a closed curve with the shape of a regular polygon. Such a regular polygon of M sides $\chi_M(0, x)$ with corners located⁷ at $x \in \mathbb{Z}$ is expected to evolve by the binormal flow to skew polygons of Mq sides at times $p/q \in \mathbb{Q}$, as suggested by numerics by Jerrard and Smets [39] and by De la Hoz and Vega [23]. Moreover, the trajectories of the corners $\chi_M(t, 0)$ were numerically proved to behave like Riemann's function $R_0(t)$ when $M \rightarrow \infty$ by De la Hoz and Vega [23] (see also De la Hoz, Kumar and Vega [22] and the corresponding video [21], a screenshot of which we show in Figure 4). The presence of Riemann's function in this context was rigorously proved by Banica and Vega [7] by taking as initial data polygonal line approximations made by regular M -polygons (looped a large amount of times) and two half-lines, for which they used the solutions constructed in their previous work [6] This approach extends to the trajectories of all locations x_0 , giving rise to R_{x_0} .

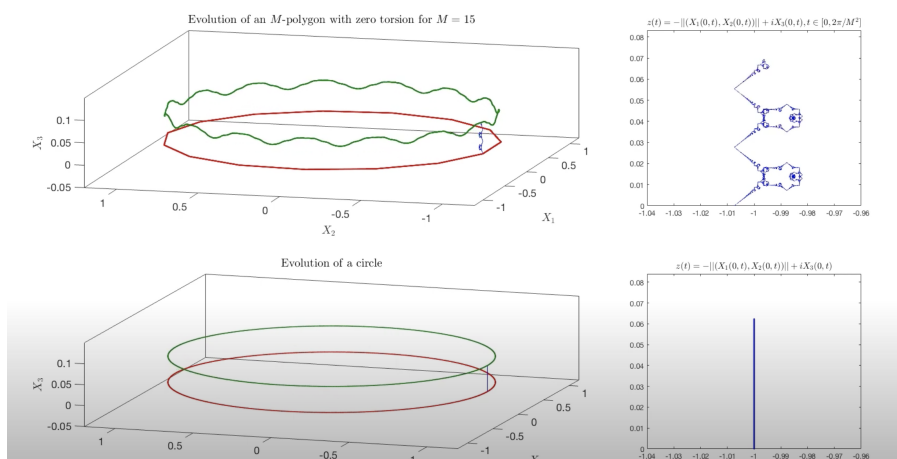


FIGURE 4. On the left: Evolution by the binormal flow of a circle and of an M -polygon with $M = 15$. On the right: the trajectory in time of the solution at $x = 0$.

⁷We see here the closed curve as being parametrized, in a periodic way, by $x \in \mathbb{R}$

3.3. Appearance of Riemann's function

Let us explain with more details how R_{x_0} arises in this context. To do so, let us first briefly state the links between the binormal flow and Schrödinger equations. One can immediately see by taking the derivative in x in (3.1) that the tangent vector T of a smooth solution χ to the binormal flow satisfies the Schrödinger map equation from \mathbb{R} to \mathbb{S}^2 , which is the Heisenberg ferromagnetic continuous model

$$T_t = T \wedge T_{xx}. \quad (3.2)$$

On the other hand, in 1972 Hasimoto [36] introduced a transform⁸ that connects explicitly the binormal flow and the 1D cubic Schrödinger equation (NLS). More precisely, for curves with non-vanishing curvature, the function

$$u(t, x) = c(t, x)e^{i \int_0^x \tau(t, y) dy},$$

where c and τ are respectively the curvature and torsion of a smooth solution to the BF, solves

$$i\partial_t u + \Delta u + \frac{1}{2}(|u|^2 - A(t))u = 0, \quad (3.3)$$

where $A(t)$ is a function that depends only on time and is defined in terms of the curvature and torsion. Koiso [41] showed in 1997 that the non-vanishing condition on the curvature can be removed by using parallel transport frames instead of Frenet frames, that is, by constructing an orthonormal basis (T, e_1, e_2) verifying

$$\begin{pmatrix} T \\ e_1 \\ e_2 \end{pmatrix}_x = \begin{pmatrix} 0 & \alpha & \beta \\ -\alpha & 0 & 0 \\ -\beta & 0 & 0 \end{pmatrix} \begin{pmatrix} T \\ e_1 \\ e_2 \end{pmatrix} \quad (3.4)$$

and

$$\begin{pmatrix} T \\ e_1 \\ e_2 \end{pmatrix}_t = \begin{pmatrix} 0 & -\beta_x & \alpha_x \\ \beta_x & 0 & -\frac{1}{2}(\alpha^2 + \beta^2 - A(t)) \\ -\alpha_x & \frac{1}{2}(\alpha^2 + \beta^2 - A(t)) & 0 \end{pmatrix} \begin{pmatrix} T \\ e_1 \\ e_2 \end{pmatrix} \quad (3.5)$$

In this case, $u = \alpha + i\beta$ solves (3.3), possibly with a different $A(t)$.

Conversely, from a smooth solution u to NLS in (3.3) with any⁹ $A(t)$, one can construct a smooth solution to the BF with tangent vector T satisfying the Schrödinger map (3.2), and frames (T, e_1, e_2) satisfying (3.4)-(3.5) with $\alpha = \text{Re}(u)$ and $\beta = \text{Im}(u)$. Thus, one could generate singularities for BF by generating singularities for smooth NLS solutions. For instance, Gutiérrez, Rivas and Vega [34] showed that the self-similar solutions of the BF are obtained from solutions of the type $t^{-1/2} e^{ix^2/4t} = e^{it\Delta} \delta$ of (3.3) with $A(t) = 1/t$. When this solution, which is smooth for $t > 0$, generates the Dirac-singularity at $t = 0$, the associated smooth BF solution generates a corner. The BF evolutions χ_M of polygonal-line approximations of M -regular polygons were constructed by Banica and Vega [6] from NLS evolutions of truncations of the Dirac comb $\sum_{|n| \lesssim M} \delta_n$. These NLS evolutions were proved to be truncations of type $\sum_{|n| \lesssim M} e^{it\Delta} \delta_n$ plus a remainder term. By using the Poisson summation formula they rewrite as truncations of type $\sum_{|n| \lesssim M} e^{in^2 t + inx}$ plus a remainder term. In view of (3.4), the derivative in time $\partial_t \chi_M = T_M \wedge \partial_x T_M$ involves the corresponding NLS solution. Consequently, the leading term of the trajectories $\chi_M(t, x_0)$ is proved to be

$$\int_0^t \sum_{n \in \mathbb{Z}} e^{in^2 \tau + inx_0} d\tau = -i\tilde{R}_{x_0}(t),$$

whence Riemann's function naturally arises.

⁸This transform can be seen as an inverse Madelung transform.

⁹This general choice is possible due to a gauge invariance.

3.4. Energy cascades

Let us briefly mention another consequence of the construction in [6]: the existence of an energy cascade for the tangent vector T , which can also be understood as an energy cascade for a linear Hamiltonian system. This was shown in [8] using the method in Section 3.3 and solutions of (3.3) with $A(t) \equiv 0$ of the type

$$u(t, x) = \frac{1}{(it)^{1/2}} e^{i \frac{|x|^2}{4t}} \overline{V} \left(\frac{1}{t}, \frac{x}{t} \right),$$

with $V(x, t)$ a smooth function that is periodic in x . Therefore, (T, e_1, e_2) solves (3.4) which, due to $u = \alpha + i\beta$, becomes

$$\begin{pmatrix} T \\ e_1 \\ e_2 \end{pmatrix}_t = \begin{pmatrix} 0 & -\operatorname{Im} u_x & \operatorname{Re} u_x \\ \operatorname{Im} u_x & 0 & -\frac{1}{2}|u|^2 \\ -\operatorname{Re} u_x & \frac{1}{2}|u|^2 & 0 \end{pmatrix} \begin{pmatrix} T \\ e_1 \\ e_2 \end{pmatrix}. \quad (3.6)$$

The matrix coefficients involve

$$|u(t, x)|^2 = \frac{1}{t} \left| V \left(\frac{1}{t}, \frac{x}{t} \right) \right|^2$$

which is a real potential, and also the derivatives in x given by

$$u_x(t, x) = i \frac{x}{2t} u(t, x) + \text{Remainder term}. \quad (3.7)$$

The first term comes from the space derivative of the exponential, and the remainder term corresponds to the space derivative hitting the smooth periodic in space function V . Therefore, with this particular choice of u , the equation for T_t in (3.6) can be seen as a linear equation with variable coefficients whose leading behaviour is given by the potential $i \frac{x}{2t} u$. The multiplication by $i \frac{x}{2t}$ creates a travelling wave in Fourier space. We refer to Theorem 1.1 in [8] for the details.

This phenomenon is reminiscent of the works of Apolinário et al. [2, 3] where they proposed abstract linear equations that mimic the phenomenology of energy cascades when the external force is a statistically homogeneous and stationary stochastic process. Indeed, these equations have a potential of the type icx with $c \in \mathbb{R}$ (see (2.2) in [2]), independent of time. Existence of energy cascades for linear systems have been also proved by Colin de Verdière and Saint-Raymond in [18].

4. Sketch of the proof of Theorem 1

In this last section we give an overview of the proof of Theorem 1 for $\alpha \in [1/2, 3/4]$. Further details can be found in [5]. To determine the spectrum of singularities of R_{x_0} we first estimate variations near rational t . This will allow to understand the variations near irrationals, depending on how well they can be approximated by rationals. By doing so, we will capture every iso-Hölder set between a larger set \mathbf{A} and a strictly smaller subset of irrationals \mathbf{B} defined by a constrained Diophantine condition that depends on x_0 . The Hausdorff dimension of the larger set \mathbf{A} is settled directly by the Jarník-Besicovitch theorem. The Hausdorff dimension of the smaller set \mathbf{B} cannot be obtained directly with the arguments that Jaffard [37] and Chamizo and Ubis [16] used for $x_0 = 0$, where the Diophantine condition is just a parity condition on the denominators. Instead, we will use first the Duffin-Schaeffer theorem [25, 42] to compute the Lebesgue measure of the sets \mathbf{B} . Once we know that, since these sets are limsup of balls, we will use the Mass Transference Principle [13] to give a lower bound for their Hausdorff dimension¹⁰.

¹⁰Which will depend on how much the balls must be dilated so that the limsup of such dilated balls has Lebesgue measure 1.

4.1. Variation of R_{x_0} at rationals

To compute the behavior of R_{x_0} around a rational $p/q \in \mathbb{Q}$, add the $n = 0$ term in the sum, split it modulo q , and use the Poisson summation formula to get

$$\begin{aligned} R_{x_0}\left(\frac{p}{q} + h\right) - R_{x_0}\left(\frac{p}{q}\right) &= \sum_{n \in \mathbb{Z}} e^{2\pi i n^2 \frac{p}{q}} \frac{e^{2\pi i n^2 h} - 1}{n^2} e^{2\pi i n x_0} - 2\pi i h \\ &= \frac{\sqrt{h}}{q} \sum_{m \in \mathbb{Z}} G(p, m_{x_0, q} + m, q) F\left(\frac{\text{dist}(x_0, \frac{\mathbb{Z}}{q}) - \frac{m}{q}}{\sqrt{h}}\right) - 2\pi i h, \end{aligned}$$

where $\text{dist}(x_0, \frac{\mathbb{Z}}{q}) = x_0 - \frac{m_{x_0, q}}{q}$ and $F(x) = \mathcal{F}\left(\frac{e^{2\pi i \xi^2} - 1}{\xi^2}\right)(x) = O\left(\frac{1}{x^2}\right)$ with $F(0) \neq 0$. Also,

$$G(p, b, q) = \sum_{r=0}^{q-1} e^{2\pi i \frac{p r^2 + b r}{q}}$$

are Gauss sums whose modulus is \sqrt{q} except when q is even and $q/2$ and b have different parity, in which case it is zero. Due to the decay of F , the leading term is $m = 0$, so

$$R_{x_0}\left(\frac{p}{q} + h\right) - R_{x_0}\left(\frac{p}{q}\right) = \frac{\sqrt{h}}{q} G(p, m_{x_0, q}, q) F\left(\frac{\text{dist}(x_0, \frac{\mathbb{Z}}{q})}{\sqrt{h}}\right) - 2\pi i h + O(\min\{\sqrt{q}h, q^{\frac{3}{2}}h^{\frac{3}{2}}\}).$$

From here, we obtain a general upper bound valid for all x_0 given by

$$\left| R_{x_0}\left(\frac{p}{q} + h\right) - R_{x_0}\left(\frac{p}{q}\right) \right| \lesssim \frac{\sqrt{h}}{\sqrt{q}} + h + O(\min\{\sqrt{q}h, q^{\frac{3}{2}}h^{\frac{3}{2}}\}). \quad (4.1)$$

On the other hand, if $G(p, m_{x_0, q}, q) \neq 0$ and $\text{dist}(x_0, \frac{\mathbb{Z}}{q}) = 0$, we get

$$R_{x_0}\left(\frac{p}{q} + h\right) - R_{x_0}\left(\frac{p}{q}\right) \simeq \frac{\sqrt{h}}{\sqrt{q}} + ih + O(\min\{\sqrt{q}h, q^{\frac{3}{2}}h^{\frac{3}{2}}\}). \quad (4.2)$$

In particular, if $x_0 = \frac{p}{Q} \in \mathbb{Q}$, these conditions are satisfied for $q \in 4Q\mathbb{N}$, so

$$R_{P/Q} \in \mathcal{C}^{1/2}(p/q) \quad \text{if } q \in 4Q\mathbb{N}. \quad (4.3)$$

4.2. Upper and lower bounds for Hölder regularity at irrationals

To obtain a lower bound for Hölder regularity at an irrational t , we start by recalling that the exponent of irrationality of t is

$$\mu(t) = \sup\{\mu > 0 : |t - \frac{p}{q}| \leq \frac{1}{q^\mu} \text{ for infinitely many coprime pairs } (p, q) \in \mathbb{N} \times \mathbb{N}\}.$$

The approximations by continuous fractions of t , denoted by p_n/q_n , satisfy

$$\left| t - \frac{p_n}{q_n} \right| = \frac{1}{q_n^{\mu_n}} \quad \text{and} \quad \mu(t) = \limsup_{n \rightarrow \infty} \mu_n.$$

Since $p_n/q_n \rightarrow t$, we have that

$$\forall h > 0, \quad \exists n \in \mathbb{N} \quad : \quad \left| t - \frac{p_n}{q_n} \right| \leq h \leq \left| t - \frac{p_{n-1}}{q_{n-1}} \right|. \quad (4.4)$$

We use (4.1), (4.4) and the property $|t - p_{n-1}/q_{n-1}| \simeq (q_n q_{n-1})^{-1}$ to estimate

$$\begin{aligned}
|R_{x_0}(t+h) - R_{x_0}(t)| &\leq \left| R_{x_0}\left(\frac{p_n}{q_n} + \left(t - \frac{p_n}{q_n} + h\right)\right) - R_{x_0}\left(\frac{p_n}{q_n}\right) \right| \\
&\quad + \left| R_{x_0}\left(\frac{p_n}{q_n} + \left(t - \frac{p_n}{q_n}\right)\right) - R_{x_0}\left(\frac{p_n}{q_n}\right) \right| \\
&\lesssim \frac{\sqrt{h}}{\sqrt{q_n}} + h + \min\{\sqrt{q_n}h, q_n^{\frac{3}{2}}h^{\frac{3}{2}}\} \\
&\lesssim h^{\frac{1}{2} + \frac{1}{2\mu_n}} + h^{\frac{1}{2} + \frac{1}{2\mu_{n-1}}} \\
&\lesssim h^{\frac{1}{2} + \frac{1}{2\mu} - \delta},
\end{aligned}$$

which holds for all $\delta > 0$. Thus, the Hölder exponent of R_{x_0} at t satisfies

$$\alpha_{R_{x_0}}(t) \geq \frac{1}{2} + \frac{1}{2\mu(t)}, \quad \forall t \notin \mathbb{Q}. \quad (4.5)$$

To obtain an upper bound for Hölder regularity at irrational t , we shall fix from now on $x_0 = \frac{P}{Q} \in \mathbb{Q}$ and we shall use the poor regularity of $R_{P/Q}$ at the rationals specified in (4.3), i.e. with denominator in $4Q\mathbb{N}$. Indeed, consider the irrationals well approximated by rationals with denominator restricted to $4Q\mathbb{N}$,

$$\mathbf{A}_{\mu, Q} = \left\{ t \notin \mathbb{Q} : \left| t - \frac{p}{q} \right| \leq \frac{1}{q^\mu} \text{ for infinitely many coprime pairs } (p, q) \in \mathbb{N} \times 4Q\mathbb{N} \right\}.$$

In particular

$$t \in \mathbf{A}_{\mu, Q} \implies \mu \leq \mu(t) = \sup\{\nu : t \in \mathbf{A}_\nu\},$$

where

$$\mathbf{A}_\nu = \left\{ t \notin \mathbb{Q} : \left| t - \frac{p}{q} \right| \leq \frac{1}{q^\nu} \text{ for infinitely many coprime pairs } (p, q) \in \mathbb{N} \times \mathbb{N} \right\}.$$

For $t \in \mathbf{A}_{\mu, Q}$, we can pick $(p_n, q_n) \in \mathbb{N} \times 4Q\mathbb{N}$ and define μ_n such that

$$\frac{1}{q_n^{\mu_n}} = \left| t - \frac{p_n}{q_n} \right| \leq \frac{1}{q_n^\mu}.$$

We set $h_n = t - \frac{p_n}{q_n}$ and we use (4.2) to get the lower estimate

$$|R_{x_0}(t+h_n) - R_{x_0}(t)| = \left| R_{x_0}\left(\frac{p_n}{q_n}\right) - R_{x_0}\left(\frac{p_n}{q_n} + h_n\right) \right| \gtrsim \frac{\sqrt{h_n}}{\sqrt{q_n}} = h_n^{\frac{1}{2} + \frac{1}{2\mu_n}} \geq h_n^{\frac{1}{2} + \frac{1}{2\mu}}.$$

Therefore, by combining this with (4.5) we obtain upper and lower bounds for the Hölder regularity at irrationals of $\mathbf{A}_{\mu, Q}$ given by

$$\frac{1}{2} + \frac{1}{2\mu(t)} \leq \alpha_{R_{x_0}}(t) \leq \frac{1}{2} + \frac{1}{2\mu}, \quad \forall t \in \mathbf{A}_{\mu, Q}. \quad (4.6)$$

4.3. Measuring the iso-Hölder sets

In (4.6) the Hölder exponent would be completely determined if $\mu(t) = \mu$. However, this is not the case for all $t \in \mathbf{A}_{\mu, Q}$. To fix this, we shall remove the points where the Hölder exponent is larger than μ by introducing the sets

$$\mathbf{B}_{\mu, Q} = \mathbf{A}_{\mu, Q} \setminus \left(\bigcup_{\epsilon > 0} \mathbf{A}_{\mu+\epsilon} \right).$$

From $\mathbf{B}_{\mu, Q} \subset \mathbf{A}_\mu \setminus \left(\bigcup_{\epsilon > 0} \mathbf{A}_{\mu+\epsilon} \right)$ and the definition of $\mu(t)$, we get that

$$t \in \mathbf{B}_{\mu, Q} \implies \mu(t) = \mu.$$

Therefore, by (4.6) and by the combination of (4.5) with $\mu(t) = \sup\{\nu : t \in \mathbf{A}_\nu\}$ we get

$$\mathbf{B}_{\mu,Q} \subset \left\{ t : \alpha_{R_{x_0}}(t) = \frac{1}{2} + \frac{1}{2\mu} \right\} \subset \mathbf{A}_{\mu-\epsilon}, \quad \forall \epsilon > 0. \quad (4.7)$$

Since Theorem 1 claims that

$$\dim_{\mathcal{H}} \left\{ t : \alpha_{R_{x_0}}(t) = \frac{1}{2} + \frac{1}{2\mu} \right\} = \frac{2}{\mu},$$

and since $\dim_{\mathcal{H}} \mathbf{A}_\nu = \frac{2}{\nu}$ for $\nu \geq 2$ by the Jarník-Besicovitch theorem, it suffices to show

$$\dim_{\mathcal{H}} \mathbf{B}_{\mu,Q} \geq \frac{2}{\mu}.$$

Since $\mathcal{H}^{\frac{2}{\mu}}(\mathbf{A}_{\mu+\frac{1}{n}}) = 0$ for all $n \in \mathbb{N}$, we can write

$$\mathcal{H}^{\frac{2}{\mu}}(\mathbf{B}_{\mu,Q}) = \mathcal{H}^{\frac{2}{\mu}}(\mathbf{A}_{\mu,Q}) - \lim_{n \rightarrow \infty} \mathcal{H}^{\frac{2}{\mu}}(\mathbf{A}_{\mu+\frac{1}{n}}) = \mathcal{H}^{\frac{2}{\mu}}(\mathbf{A}_{\mu,Q}),$$

so it is enough to prove $\mathcal{H}^{\frac{2}{\mu}}(\mathbf{A}_{\mu,Q}) > 0$. We will actually prove

$$\mathcal{H}^{\frac{2}{\mu}}(\mathbf{A}_{\mu,Q}) = \infty, \quad (4.8)$$

which will complete the proof.

First, we use the Duffin-Schaeffer theorem [42], which states that if

$$\sum_{q=1}^{\infty} \psi(q) \varphi(q) = \infty, \quad (4.9)$$

where φ is Euler's totient function¹¹ and ψ is an arbitrary function, then the set

$$\mathbf{A}_\psi = \left\{ t : \left| t - \frac{p}{q} \right| \leq \psi(q) \text{ for infinitely many coprime pairs } (p, q) \in \mathbb{N} \times \mathbb{N} \right\}$$

has Lebesgue measure 1. The function $\psi(q) := \frac{\mathbb{1}_{4\mathbb{Q}\mathbb{N}}(q)}{q^2}$ satisfies the hypothesis (4.9) and $\mathbf{A}_\psi = \mathbf{A}_{2,Q}$, so the Duffin-Schaeffer theorem implies

$$\mathcal{L}(\mathbf{A}_{2,Q}) = 1.$$

Once we know this, we use the Mass Transference Principle of Beresnevich and Velani [13], which says that if $B(x_n, r_n)$ is a sequence of balls in $[0, 1]^d$ with $r_n \rightarrow 0$, and if for some $\alpha < d$ we have

$$\mathcal{L}\left(\limsup_n B(x_n, r_n^{\alpha/d})\right) = 1,$$

then

$$\dim_{\mathcal{H}}\left(\limsup_n B(x_n, r_n)\right) \geq \alpha, \quad \text{and} \quad \mathcal{H}^\alpha\left(\limsup_n B(x_n, r_n)\right) = \infty.$$

In our case $d = 1$, since we have obtained

$$\begin{aligned} 1 = \mathcal{L}(\mathbf{A}_{2,Q}) &= \mathcal{L}\left(\limsup_q \bigcup_{p \leq q, (p,q)=1} B\left(\frac{p}{q}, \frac{\mathbb{1}_{4\mathbb{Q}\mathbb{N}}(q)}{q^2}\right)\right) \\ &= \mathcal{L}\left(\limsup_q \bigcup_{p \leq q, (p,q)=1} B\left(\frac{p}{q}, \left(\frac{\mathbb{1}_{4\mathbb{Q}\mathbb{N}}(q)}{q^\mu}\right)^{2/\mu}\right)\right), \end{aligned} \quad (4.10)$$

applying the result above with $\alpha = 2/\mu$ we get

$$\mathcal{H}^{\frac{2}{\mu}}\left(\limsup_q \bigcup_{p \leq q, (p,q)=1} B\left(\frac{p}{q}, \frac{\mathbb{1}_{4\mathbb{Q}\mathbb{N}}(q)}{q^\mu}\right)\right) = \mathcal{H}^{\frac{2}{\mu}}(\mathbf{A}_{\mu,Q}) = \infty,$$

¹¹Euler's totient function is $\varphi(q) = \#\{1 \leq m \leq q : \gcd(m, q) = 1\}$.

which is what we wanted to prove in (4.8). The proof is complete.

Bibliography

- [1] Fabien Anselmet, Yves Gagne, Emil J. Hopfinger, and Robert A. Antonia. High-order velocity structure functions in turbulent shear flows. *J. Fluid Mech.*, 140:63–89, 1984.
- [2] Gabriel B. Apolinário, Geoffrey Beck, Laurent Chevillard, Isabelle Gallagher, and Ricardo Grande. A linear stochastic model of turbulent cascades and fractional fields. *To appear in Ann. Sc. Norm. Super. Pisa Cl. Sci. (2023)*, 2023. arXiv:2301.00780.
- [3] Gabriel B. Apolinário, Laurent Chevillard, and Jean-Christophe Mourrat. Dynamical fractional and multifractal fields. *J. Stat. Phys.*, 186(1):35, 2022. Id/No 15.
- [4] Alain Arneodo and Stephane Jaffard. L’analyse multifractale des signaux. *Images des Mathématiques*, 2024.
- [5] Valeria Banica, Daniel Eceizabarrena, Andrea Nahmod, and Luis Vega. Multifractality and intermittency in the limit evolution of polygonal vortex filaments. *To appear in: Math. Ann.*, 2024. <https://doi.org/10.1007/s00208-024-02971-0>.
- [6] Valeria Banica and Luis Vega. Evolution of polygonal lines by the binormal flow. *Ann. PDE*, 6(1):53, 2020. Id/No 6.
- [7] Valeria Banica and Luis Vega. Riemann’s non-differentiable function and the binormal curvature flow. *Arch. Ration. Mech. Anal.*, 244(2):501–540, 2022.
- [8] Valeria Banica and Luis Vega. Unbounded growth of the energy density associated to the Schrödinger map and the binormal flow. *Ann. Inst. Henri Poincaré, Anal. Non Linéaire*, 39(4):927–946, 2022.
- [9] Valeria Banica and Luis Vega. New conservation laws and energy cascade for 1d cubic NLS and the Schrödinger map. *Vietnam J. Math.*, 52(4):985–999, 2024.
- [10] Julien Barral and Stéphane Seuret. The Frisch-Parisi conjecture. I: Prescribed multifractal behavior, and a partial solution. *J. Math. Pures Appl. (9)*, 175:76–108, 2023.
- [11] Julien Barral and Stéphane Seuret. The Frisch-Parisi conjecture. II: Besov spaces in multifractal environment, and a full solution. *J. Math. Pures Appl. (9)*, 175:281–329, 2023.
- [12] Jacob Bedrossian, Pierre Germain, and Benjamin Harrop-Griffiths. Vortex filament solutions of the Navier-Stokes equations. *Comm. Pure Appl. Math.*, 76(4):685–787, 2023.
- [13] Victor Beresnevich and Sanju Velani. A mass transference principle and the Duffin-Schaeffer conjecture for Hausdorff measures. *Ann. of Math. (2)*, 164(3):971–992, 2006.
- [14] Alexandre Boritchev, Daniel Eceizabarrena, and Victor Vilaça Da Rocha. Intermittency of Riemann’s non-differentiable function through the fourth-order flatness. *J. Math. Phys.*, 62(9):Paper No. 093101, 14, 2021.
- [15] Frederik Broucke and Jasson Vindas. The pointwise behavior of Riemann’s function. *J. Fractal Geom.*, 10(3-4):333–349, 2023.
- [16] Fernando Chamizo and Adrián Ubis. Multifractal behavior of polynomial Fourier series. *Adv. Math.*, 250:1–34, 2014.
- [17] Laurent Chevillard, Bernard Castaing, Alain Arneodo, Emmanuel Lévêque, Jean-François Pinton, and Stéphane G. Roux. A phenomenological theory of Eulerian and Lagrangian velocity fluctuations in turbulent flows. *Comptes Rendus. Physique*, 13(9-10):899–928, 2012.
- [18] Yves Colin de Verdière and Laure Saint-Raymond. Attractors for two-dimensional waves with homogeneous Hamiltonians of degree 0. *Commun. Pure Appl. Math.*, 73(2):421–462, 2020.
- [19] Luigi Sante Da Rios. Sul moto d’un liquido indefinito con un filetto vorticoso di forma qualunque. *Rend. Circ. Mat. Palermo*, 22:117–135, 1906.
- [20] Juan Dávila, Manuel del Pino, Monica Musso, and Juncheng Wei. Travelling helices and the vortex filament conjecture in the incompressible Euler equations. *Calc. Var. Partial Differential Equations*, 61(4):Paper No. 119, 30, 2022.
- [21] Francisco de la Hoz, Sandeep Kumar, and Luis Vega. <https://www.youtube.com/watch?v=bwbpKvqGk-o&feature=youtu.be>.
- [22] Francisco de la Hoz, Sandeep Kumar, and Luis Vega. On the evolution of the vortex filament equation for regular M -polygons with nonzero torsion. *SIAM J. Appl. Math.*, 80(2):1034–1056, 2020.
- [23] Francisco de la Hoz and Luis Vega. Vortex filament equation for a regular polygon. *Nonlinearity*, 27(12):3031–3057, 2014.
- [24] Martin Donati, Christophe Lacave, and Evelyne Miot. Dynamics of helical vortex filaments in non viscous incompressible flows. *Preprint*, 2024. arXiv:2403.00389.
- [25] Richard J. Duffin and Albert C. Schaeffer. Khintchine’s problem in metric Diophantine approximation. *Duke Math. J.*, 8:243–255, 1941.

- [26] Daniel Eceizabarrena. Geometric differentiability of Riemann’s non-differentiable function. *Adv. Math.*, 366:107091, 39, 2020.
- [27] Daniel Eceizabarrena. On the Hausdorff dimension of Riemann’s non-differentiable function. *Trans. Amer. Math. Soc.*, 374(11):7679–7713, 2021.
- [28] Daniel Eceizabarrena and Victor Vilaça Da Rocha. An analytical study of flatness and intermittency through Riemann’s nondifferentiable functions. *SIAM J. Math. Anal.*, 54(3):3575–3608, 2022.
- [29] Marco Antonio Fontelos and Luis Vega. Evolution of viscous vortex filaments and desingularization of the biot-savart integral. *Preprint*. arXiv:2311.12246.
- [30] Thierry Gallay and Vladimír Sverák. Vanishing viscosity limit for axisymmetric vortex rings. *Invent. Math.*, 237(1):275–348, 2024.
- [31] Joseph Gerver. The differentiability of the Riemann function at certain rational multiples of π . *Amer. J. Math.*, 92:33–55, 1970.
- [32] Joseph Gerver. More on the differentiability of the Riemann function. *Amer. J. Math.*, 93:33–41, 1971.
- [33] Fernando F. Grinstein and Carl R. De Vore. Dynamics of coherent structures and transition to turbulence in free square jets. *Physics of Fluids*, 8(5):1237–1251, 1996.
- [34] Susana Gutiérrez, Judith Rivas, and Luis Vega. Formation of singularities and self-similar vortex motion under the localized induction approximation. *Comm. Partial Differential Equations*, 28(5-6):927–968, 2003.
- [35] Godfrey H. Hardy. Weierstrass’s non-differentiable function. *Trans. Amer. Math. Soc.*, 17(3):301–325, 1916.
- [36] Hidenori Hasimoto. A soliton on a vortex filament. *J. Fluid Mech.*, 51:477–485, 1972.
- [37] Stephane Jaffard. The spectrum of singularities of Riemann’s function. *Rev. Mat. Iberoamericana*, 12(2):441–460, 1996.
- [38] Robert L. Jerrard and Christian Seis. On the vortex filament conjecture for Euler flows. *Arch. Ration. Mech. Anal.*, 224(1):135–172, 2017.
- [39] Robert L. Jerrard and Didier Smets. On the motion of a curve by its binormal curvature. *J. Eur. Math. Soc. (JEMS)*, 17(6):1487–1515, 2015.
- [40] Lev Kapitanski and Igor Rodnianski. Does a quantum particle know the time? In *Emerging applications of number theory (Minneapolis, MN, 1996)*, volume 109 of *IMA Vol. Math. Appl.*, pages 355–371. Springer, New York, 1999.
- [41] Norihito Koiso. The vortex filament equation and a semilinear Schrödinger equation in a Hermitian symmetric space. *Osaka J. Math.*, 34(1):199–214, 1997.
- [42] Dimitris Koukoulopoulos and James Maynard. On the Duffin-Schaeffer conjecture. *Ann. of Math. (2)*, 192(1):251–307, 2020.
- [43] Stéphane Seuret and Adrián Ubis. Local L^2 -regularity of Riemann’s Fourier series. *Ann. Inst. Fourier (Grenoble)*, 67(5):2237–2264, 2017.
- [44] Weixiao Shen. Hausdorff dimension of the graphs of the classical Weierstrass functions. *Math. Z.*, 289(1-2):223–266, 2018.
- [45] Kuniaki Todoya and Fazle Hussain. A study of the vortical structures of noncircular jets. *Trans. Japan Soc. Mech. Eng. Ser. B*, 55(514):1542–1545, 1989.

VALERIA BANICA
 Sorbonne Université, Université Paris Cité, CNRS,
 INRIA, Laboratoire Jacques-Louis Lions, LJLL,
 F-75005 Paris, France
 Valeria.Banica@math.cnrs.fr

DANIEL ECEIZABARRENA
 BCAM - Basque Center for Applied Mathematics
 Bilbao, Spain
 deceizabarrena@bcamath.org

ANDREA R. NAHMOD
 Department of Mathematics and Statistics
 University of Massachusetts Amherst
 710 N Pleasant St, Amherst, MA 01003, USA
 nahmod@umass.edu

LUIS VEGA
 Department of Mathematics
 University of Basque Country
 Apdo 644, 48080 Bilbao, Spain
 lvega@bcamath.org